

FOSSIL PLANTS AS INDICATORS OF THE PHANEROZOIC GLOBAL CARBON CYCLE

D.J. Beerling and D.L. Royer

Department of Animal and Plant Sciences, University of Sheffield, Sheffield S10 2TN, United Kingdom; e-mail: d.j.beerling@sheffield.ac.uk

Key Words atmospheric CO₂, stable carbon isotopes, leaf fossils, stomata

■ **Abstract** Developments in plant physiology since the 1980s have led to the realization that fossil plants archive both the isotopic composition of atmospheric CO₂ and its concentration, both critical integrators of carbon cycle processes through geologic time. These two carbon cycle signals can be read by analyzing the stable carbon isotope composition ($\delta^{13}\text{C}$) of fossilized terrestrial organic matter and by determining the stomatal characters of well-preserved fossil leaves, respectively. We critically evaluate the use of fossil plants in this way at abrupt climatic boundaries associated with mass extinctions and during times of extreme global warmth. Particular emphasis is placed on evaluating the potential to extract a quantitative estimate of the $\delta^{13}\text{C}$ of atmospheric CO₂ because of the key role it plays in understanding the carbon cycle. We critically discuss the use of stomatal index and stomatal ratios for reconstructing atmospheric CO₂ levels, especially the need for adequate replication, and present a newly derived CO₂ record for the Mesozoic that supports levels calculated from geochemical modeling of the long-term carbon cycle. Several suggestions for future research using stable carbon isotope analyses of fossil terrestrial organic matter and stomatal measurements are highlighted.

INTRODUCTION

Earth history is characterized by major changes in the global carbon cycle reflecting variations in the relative strength of the sources and sinks for inorganic and organic carbon (Sundquist & Broecker 1985). On geologic timescales, CO₂ is supplied to the atmosphere by volcanism and metamorphism and removed by silicate weathering reactions driven primarily by tectonic uplift, climate, and the presence and distribution of land plants (Berner 1997, 1998). Superimposed upon these long-term changes in carbon cycling are more subtle short-term variations resulting from shifts in the activity of the terrestrial and marine biospheres (Falkowski et al. 2000). The direct effect of carbon strategy in land plants and soils on atmospheric CO₂ levels over millions of years is minor, however, because at any one time the total quantity of carbon stored is small (~2000–3000 Gt, where

1 Gt = 10^{15} g) compared with the amount of carbon in the oceans ($\sim 38,000$ Gt) and sedimentary rocks (60×10^6 Gt C) (Walker 1994).

Carbon fixation by terrestrial ecosystems at the global scale in the distant past is primarily determined by substrate availability (i.e., atmospheric CO_2 concentration) and climate (Beerling 2000). Climate directly influences plant physiological processes and exerts a secondary, but important, control on productivity through its effects on soil carbon and nitrogen dynamics (McGuire et al. 1992). Therefore, a tight coupling exists between climate, atmospheric CO_2 , and productivity. Photosynthetic primary production in vascular plants with the C_3 photosynthetic pathway utilizes the enzyme Rubisco (ribulose-1,5-bisphosphate carboxylase/oxygenase) to fix inorganic carbon from the atmosphere. During photosynthetic CO_2 uptake, a kinetic isotopic fractionation effect occurs, which combines with the action of stomatal activities (Farquhar et al. 1982, 1989) to determine the fractionation between atmospheric CO_2 and the C_3 terrestrial carbon reservoir (Lloyd & Farquhar 1994). The isotopic abundance of terrestrial organic matter reflects this fractionation plus the ^{13}C content of the source (atmospheric) CO_2 , which, under equilibrium conditions, reflects the isotopic composition of seawater. It follows that shifts in the isotopic composition of terrestrial carbon pool integrate changes in the inorganic carbon reservoir and the effects of climate on ocean-atmosphere, biosphere-atmosphere isotopic exchanges.

Virtually all of the carbon fixed by vascular land plants via photosynthesis passes through stomata. The stomatal conduits are small ($\sim 10^2$ μm in length), but the fluxes of CO_2 and water vapor exchanged through them at the global scale are large (Gt). For the present-day, the annual CO_2 flux represents approximately 40% of the total atmospheric mass (Ciais et al. 1997). Stomata therefore play a part in regulating the exchange of CO_2 and water vapor between the land surface and the surrounding atmosphere. The pivotal role of stomata in the terrestrial carbon cycle indicates that the fossil record of changes in the stomatal characters of land plant leaves through geologic time will provide information about the ancient carbon cycle. Observations on modern plants have demonstrated from historical materials, and in controlled environment experiments, an inverse relationship between atmospheric CO_2 levels and the stomatal density (numbers per area of leaf) and index (the percentage of epidermal cells that are stomata) (Woodward 1987). When applied with suitable controls on taxonomy, replication, and taphonomic setting, this relationship provides a basis for reading a quantitative CO_2 signal from the stomatal index of fossil leaves (Beerling 1999, Royer et al. 2001a, Beerling & Royer 2002). Reconstruction of atmospheric CO_2 levels in this way (van der Burgh et al. 1993, Kürschner et al. 1996, Rundgren & Beerling 1999, Wagner et al. 1999, Royer et al. 2001b) retrieves information on the mass of carbon in the atmospheric reservoir. Furthermore, these CO_2 estimates can be used to calculate the extent of CO_2 -related climate forcing for comparison with independent oxygen isotope-derived paleoclimate curves (e.g., Zachos et al. 2001) and other proxy measures of paleoclimate.

The fossil record of land plants therefore represents a sensitive and detailed archive of past changes in the isotopic composition of the inorganic marine and atmospheric carbon reservoirs and the mass of carbon in the atmosphere. Integrated into the isotopic signature of terrestrial organic matter is a climatic signal. We focus on the interpretation and analysis of these features of the fossil record because, in our opinion, they represent the most effective deployment of fossil specimens for deciphering past changes in the global carbon cycle on a Phanerozoic timescale. We recognize, of course, that the rise and spread of vascular land plants themselves played a major role in the trajectory of atmospheric CO₂ levels during the Paleozoic through their effects on silicate rock weathering and organic carbon burial (Berner 1997, Algeo & Scheckler 1998).

In this review, we critically examine the use and interpretation of variations in the stable carbon isotope composition of fossil plant materials and the stomatal indices of fossil leaves. In particular, we evaluate the use of carbon isotope excursions for cross-correlating marine and terrestrial sections at abrupt climatic boundaries associated with mass extinctions, and rigorously assess the important suggestion (Arens et al. 2000) that plant fossils provide a means of directly estimating the isotopic composition of atmospheric CO₂. Key constraints on the use of stomatal indices as indicators of paleoatmospheric CO₂ concentration are discussed, and we then proceed to examine their utility for reconstructing patterns of CO₂ change during the Mesozoic and early Tertiary. We close with some possible future directions for isotopic and stomatal research, in particular the emerging technique of compound-specific isotopic analyses of fossil molecules (Hinrichs et al. 2001) and the use of stomatal indices as paleoelevation barometers.

CARBON ISOTOPE COMPOSITION OF FOSSIL PLANTS

Theory

The isotopic composition of C₃ vascular land plant materials ($\delta^{13}C_p$) integrates, over the lifetime of the tissue, the isotopic composition of the inorganic source CO₂ ($\delta^{13}C_a$) and the effects of climate and soils on leaf metabolic processes (Farquhar et al. 1982). It is well described by the widely validated model (Farquhar et al. 1982, Farquhar & Lloyd 1993):

$$\delta^{13}C_p = \delta^{13}C_a - a - (b - a) \times \frac{c_{st}}{c_a}, \quad (1)$$

where a (4.4‰) accounts for the fractionation occurring as CO₂ molecules diffuse through free air and the stomatal pores, b is the kinetic fractionation occurring during CO₂ fixation by Rubisco (27‰–30‰) (Guy et al. 1993) reflecting the sensitivity of the enzyme to the atomic masses of ¹²CO₂/¹³CO₂ molecules, and c_{st}/c_a is the ratio of CO₂ partial pressures in the substomatal cavity (sometimes referred to as the “intercellular CO₂ partial pressure”) and the atmosphere. The c_{st}/c_a term is controlled by the balance between CO₂ demand by the photosynthesis in the

mesophyll and CO₂ supply by diffusion through stomata. It is important to note that the isotopic composition of plant materials reflects an assimilation-weighted average of the discrimination occurring over the entire growth period and the effects of secondary metabolism and export of carbon compounds during the life of the leaf. Furthermore, Equation 1 only represents an approximation of the more complete expression required to account for all of the various processes with differing isotopic discriminations occurring during CO₂ assimilation (Farquhar & Lloyd 1993). Nevertheless, concurrent measurements have confirmed that c_{st}/c_a strongly influences the extent of carbon isotope discrimination by leaves (Evans et al. 1986), in agreement with theory (Farquhar et al. 1982).

Any climatically dynamic period in Earth history influencing the long-term or short-term carbon cycle will tend to force isotopic shifts in the atmospheric carbon pool (Kump & Arthur 1999). The relationship between $\delta^{13}\text{C}_p$ and $\delta^{13}\text{C}_a$ described by Equation 1 therefore indicates that such events will exert an effect on $\delta^{13}\text{C}_p$ and, assuming no major diagenetic impacts, will be preserved in the fossil record (Beerling 1997). Additionally, shifts in the isotopic composition of plants may be transferred to that of the tooth enamel of herbivorous grazers (DeNiro & Epstein 1978) and to paleosol carbonates (Cerling 1991). This cascade effect through the ecosystem trophic levels increases the likelihood of detecting a marine signal on land. It was recognized early on that the rapid transfer of isotopic signals between the marine and terrestrial carbon reservoirs offered an important means of developing a chemostratigraphic tool that could be readily exploited for correlating continental and marine events (Thackeray et al. 1990, Koch et al. 1992, Stott et al. 1996, Gröcke 1998). Theory dictates that abrupt changes in sedimentary carbon-isotope abundance occur in response to rapid climatic transitions (Kump & Arthur 1999), themselves likely to induce an abrupt biotic response, as often observed in the Phanerozoic fossil record (Crowley & North 1988).

The Paleocene/Eocene Boundary, 55 Million Years Ago

A classic example of this line of reasoning comes from detailed work on an unusually abrupt warming of the surface and deep oceans during major benthic extinctions across the Paleocene/Eocene (P/E) boundary (Kennett & Stott 1991). Koch et al. (1992) postulated that the brief aberration in near-surface planktonic foraminifera $\delta^{13}\text{C}$ across the P/E boundary (Kennett & Stott 1991) would be recorded as a corresponding shift in the $\delta^{13}\text{C}$ of pedogenic carbonates in continental paleosols and the tooth enamel of mammalian browsers. Isotopic analyses of these continental materials from a detailed stratigraphic sequence in the Bighorn Basin (Wyoming, U.S.A.) indicated that the extraordinary negative excursion shown by the marine data was indeed evident with similar characteristics (Koch et al. 1992, 1995). The isotopic signal, marking an episode of rapid climate warming 55.5 mya, provided a datum for precise correlation between marine and terrestrial records. Subsequently, the short-term excursion has been detected in a worldwide set of marine localities, as well as terrestrial plant remains from numerous

sites (Kaiho et al. 1996, Stott et al. 1996, Beerling & Jolley 1998), indicating the validity of the approach. A leading hypothesis, invoked to explain the magnitude and timescale of this isosynchronous event, is the injection of isotopically light CH_4 into the ocean-atmosphere system (-60%) from the decomposition of sedimentary methane hydrates (Dickens et al. 1995, 1997).

The Cretaceous/Tertiary Boundary 65 Million Years Ago

In a similar manner to the P/E studies, the $\delta^{13}\text{C}$ excursion first reported in marine sections worldwide across the Cretaceous/Tertiary (K/T) boundary mass extinction event (e.g., Zachos et al. 1989, D'Hondt et al. 1998) has subsequently been detected in land plant carbon isotope records (Schimmelmann & DeNiro 1984, Arinobu et al. 1999, Arens & Jahren 2000, Beerling et al. 2001). An aspect of the work developed for this boundary has been the parallel examination of the duration of the nonmarine $\delta^{13}\text{C}$ excursion in relation to the pattern of ecosystem recovery in the Southwestern U.S., the latter determined from independent paleobotanical analyses (Beerling et al. 2001). Across the K/T boundary, $\delta^{13}\text{C}_p$ values reflect a $\delta^{13}\text{C}_a$ signal primarily driven by a shutdown or reduction in the uptake of $^{12}\text{CO}_2$ by phytoplankton because of extinctions in the oceans. There was probably also a contribution of isotopically negative carbon from a pulse of biomass burning (Wolbach et al. 1988). In this case, $\delta^{13}\text{C}_p$ is effectively a tracer for the collapse and recovery of marine primary production.

Comparison of both $\delta^{13}\text{C}_p$ and the results from palynological and cuticle analyses made on samples from the same nonmarine section allow a direct comparison of the relative recovery patterns of marine or terrestrial ecosystems across the K/T boundary mass extinction event (Beerling et al. 2001). The combined geochemical and paleobotanical analyses suggest terrestrial ecosystem structure recovered ahead of the negative $\delta^{13}\text{C}_p$ excursion. This differential pattern indicates marine primary production had not yet recovered (Beerling et al. 2001), perhaps because of the greater severity of extinctions in the marine realm (D'Hondt et al. 1998). An interesting feature to emerge, however, was the continued delay in the recovery of terrestrial plant biodiversity, as determined from dispersed cuticle studies (Beerling et al. 2001). This finding supports the notion that biodiversity recovery following a major environmental perturbation may take millions of years (Kirchner & Weil 2000).

The Triassic/Jurassic Boundary, 200 Million Years Ago

The Triassic/Jurassic boundary is marked by one of the largest mass extinction events in Earth history (Sepkoski 1996). Until recently, relatively little information was known about the global carbon cycle at this time because of the relative paucity of complete marine sections not subjected to significant diagenetic alteration and reworking of materials. An initial series of $\delta^{13}\text{C}_p$ measurements, made on terrestrial plant leaves from a lacustrine section in Greenland (McElwain et al. 1999), detected an isotopic excursion not yet identified in the marine realm. Subsequently,

independent detailed isotopic analyses of bulk marine organic matter and carbonates identified it in sections on the Queen Charlotte Islands, British Columbia, Canada (Ward et al. 2001) and Csővár, Hungary (Pálffy et al. 2001). This represents one of the few (the only?) examples of an isotopic signal being detected first on the land and then in the seas.

These reports provide accumulating evidence for a possible global isotopic anomaly at the boundary between the Triassic and Jurassic periods (Beerling 2002), a feature in common with the Permian/Triassic (Thackeray et al. 1990, Broecker & Peacock 1999), Cretaceous/Tertiary, and Paleocene/Eocene boundaries (see above). The minus 2‰ excursion across the boundary seen in bulk organic matter from British Columbia was stratigraphically restricted, defined by multiple samples, and well above the background variation of the rest of the section (Ward et al. 2001). In Hungary, a parallel negative excursion has been found in carbonates and marine organic matter of 3.5 and 2‰ (Pálffy et al. 2001). Taken together, the Hungarian isotope data imply an enrichment in the total exchangeable carbon reservoir in ^{12}C . It critically remains to determine the mechanisms driving these isotopic shifts. The two most likely candidates echo those postulated to have operated at the K/T and P/E boundaries respectively: reductions in marine primary production and the release of isotopically carbon light methane from hydrate reservoirs (Pálffy et al. 2001).

Secular Trends in Mesozoic $\delta^{13}\text{C}_p$ Records

An emerging feature of isotopic investigations on fossil materials is the use of fossil wood fragments and the coalified remains of highly lignified tissues as tracers for isotopic signals in the atmospheric CO_2 reservoir (Gröcke 1998, Gröcke et al. 1999, Hesselbo et al. 2000, Arens et al. 2000). At first sight, several problems appear to be inherent in this approach. Fossil woods from different depths in a given section vary greatly in ring thickness (diameter), an indicator of annual climate in contemporary trees. Variations in $\delta^{13}\text{C}$ between rings in modern woods, driven by inter-annual climate variation, can be large (up to several per mil) (Leavitt 1993), but remains to be quantified in fossil woods. It is uncertain how repeatable the $\delta^{13}\text{C}$ curve structure is when derived in this way. Another possible difficulty is taxonomy. Woods of different tree species differ in their $\delta^{13}\text{C}$ values by virtue of their different physiological responses to the climatic and edaphic environment (Leavitt & Long 1986, Feng 1998), indicating that taxonomy needs to be controlled for, an ideal rarely achieved.

Given these potential difficulties, it is surprising that $\delta^{13}\text{C}_p$ patterns resulting from analyses of bulk woods show trends similar to corresponding marine carbonate records (Gröcke et al. 1999, Hesselbo et al. 2000, Arens et al. 2000). Early Cretaceous woods from the Isle of Wight, U.K., for example, show a $\delta^{13}\text{C}_p$ pattern similar to the carbonate curve from Tethyan Europe, with the negative and positive excursions broadly aligning (Gröcke et al. 1999). Results of this sort suggest that inter-annual climate variability and taxonomic variation are overridden by the strength of the $\delta^{13}\text{C}_a$ signal.

Two detailed studies appear to confirm the utility of the approach. Early Jurassic woods from U.K. and Danish sites both show significant negative $\delta^{13}\text{C}_p$ excursions of over 4‰ during the Early Toarcian oceanic anoxic event (Hesselbo et al. 2000), whereas the structure of the curve from the U.K. site mirrors that obtained from $\delta^{13}\text{C}$ measurements on bulk organic matter from the same section. Another unusual isotopic anomaly has been identified by $\delta^{13}\text{C}$ analyses of Early Cretaceous bulk organic matter, coalified woody plant tissue, and cuticles from South American near-shore terrestrial sediments. These records show an abrupt negative 7‰ excursion in all of the different sets of materials, and a strong congruence with earlier $\delta^{13}\text{C}$ records from marine organic carbon and carbonates (Arens et al. 2000). The signal was not, however, apparent in the U.K. $\delta^{13}\text{C}_p$ records spanning the same period (Gröcke et al. 1999), perhaps because of differences in sampling resolution and dating controls.

All of these studies clearly indicate the value of terrestrial organic matter in documenting temporal trends in $\delta^{13}\text{C}_p$ and hold promise for tracing past variations in the global carbon cycle, particularly at times when reliable marine geochemical records are scarce. A common feature to emerge from analyses of bulk plant materials is the large magnitude of the isotopic excursions, often larger than the signal shown by marine carbonate records. The excursions are typically too large to be accounted for by volcanic CO_2 degassing (Kump & Arthur 1999). Instead, the intriguing suggestion has been made that the isotopic events reflect substantial episodic releases of isotopically light (–60‰) methane from gas hydrate reservoirs in marine continental margins (Dickens et al. 1995, 1997; Hesselbo et al. 2000; Beerling et al. 2002b; Arens et al. 2000). Improved interpretation of these important isotopic records requires greater critical evaluation of the possible sources of error involved.

Can $\delta^{13}\text{C}_a$ be Quantitatively Reconstructed from $\delta^{13}\text{C}_p$?

Experimental work with contemporary plants has shown a link between photosynthesis and stomatal conductance (Wong et al. 1979). In consequence, c_{st}/c_a tends to remain more or less independent of irradiance and temperature but decreases with increasing leaf-to-air vapor pressure deficit (VPD) (Wong et al. 1978). These observations are of relevance for interpreting changes in the $\delta^{13}\text{C}_p$ of fossils because they indicate that paleo- $\delta^{13}\text{C}_p$ shifts may be driven by differences in the set point of leaf metabolism (i.e., c_{st}/c_a ratio) and changes in $\delta^{13}\text{C}_a$. Tree ring records of extant forests show that extreme climatic events, such as summer droughts, are recorded as sharp $\delta^{13}\text{C}$ shifts in the annual growth rings (Leavitt 1993, Robertson et al. 1997, Walcroft et al. 1997, Berninger et al. 2000). Under these conditions, increased air temperatures raise the leaf-to-air VPD, inducing stomatal closure and limit photosynthesis, with an influence on isotopic fractionation (Farquhar et al. 1982). Tree ring studies therefore support the idea that a switch from a cool, wet climate to a warmer, drier one would induce a corresponding $\delta^{13}\text{C}_p$ shift, driven without any major changes in $\delta^{13}\text{C}_a$. By extension, this situation predicts that past climatic swings imposed a direct metabolic impact on $\delta^{13}\text{C}_p$.

All of the isotopic studies of fossil plant materials considered so far assume gross changes in $\delta^{13}\text{C}_p$ driven by changes in $\delta^{13}\text{C}_a$. Arens et al. (2000), however, have gone further by suggesting it is possible to predict $\delta^{13}\text{C}_a$ from $\delta^{13}\text{C}_p$ measurements on fossil plants. To achieve this aim, they investigated the correlation between $\delta^{13}\text{C}_p$ and $\delta^{13}\text{C}_a$ through a database of published observations. Although the resulting relationship had poor predictive capacity ($r^2 = 0.34$), it was suggested $\delta^{13}\text{C}_a$ could be quantitatively predicted from $\delta^{13}\text{C}_p$ measurements (Arens et al. 2000) according to the equation

$$\delta^{13}\text{C}_a = \frac{\delta^{13}\text{C}_p + 18.67}{1.1}. \quad (2)$$

This proposal is important because it potentially offers a means of reconstructing ancient values of $\delta^{13}\text{C}_a$, an indicator of past carbon cycle processes. Furthermore, $\delta^{13}\text{C}_a$ provides an important constraint on global carbon isotope mass balance budgets in historical breakdowns of the carbon cycle, and its value influences atmospheric CO_2 levels calculated from paleosol carbonate isotopic data using the reaction-diffusion model of Cerling (1991, 1992).

During abrupt paleoclimatic events, for example, across the P/E boundary (Koch et al. 1992) and during the early Cretaceous (Jahren et al. 2001), $\delta^{13}\text{C}_p$ closely tracks surface ocean and bulk marine carbonate $\delta^{13}\text{C}$ records, except that the magnitudes of the plant-based isotopic excursions are larger than the marine records by ~ 2.5 to 4.5 per mil. Given that the surface oceans and atmosphere exchange on rapid timescales, this difference is probably real and indicates some amplification of the marine signal. Several different mechanisms might be involved, including increased ecosystem respiration and the recycling of soil/plant respired CO_2 by photosynthesis (Broadmeadow & Griffiths 1993), or changes in climate altering the operational c_{st}/c_a ratio of leaves of vegetation. If these mechanisms operate, then measurements of $\delta^{13}\text{C}_p$ used in Equation 2 may result in erroneous estimates of $\delta^{13}\text{C}_a$.

A critical assumption of Equation 2 is that c_{st}/c_a remains constant over geologic time. Experimental data have not yet examined the constancy of leaf c_{st}/c_a to marked changes in climate in the long-term, and so far the predictive capacity of Equation 2 has not been adequately examined in extant plants. Therefore, we investigate its utility for predicting $\delta^{13}\text{C}_a$ from a series of $\delta^{13}\text{C}_p$ measurements made on tree leaves sampled between 1820 AD and 1980 AD and early Tertiary fossil *Ginkgo* leaves spanning nearly 10 Ma (Royer et al. 2001b).

We first consider the prediction of historical variations in $\delta^{13}\text{C}_a$ using $\delta^{13}\text{C}_p$ measurements of leaves for a range of temperate tree species growing in southern England over the past 200 years of anthropogenically driven atmospheric CO_2 increases (Woodward 1993; Beerling 1996, 1997). The advantage of this test is that instrumental measurements of $\delta^{13}\text{C}_a$ are available (post 1958) (Keeling et al. 1995) together with a well-dated preinstrumental record of $\delta^{13}\text{C}_a$ data from ice core studies (Friedli et al. 1986). The $\delta^{13}\text{C}_p$ measurements show a general trend with time toward more negative values by nearly 4‰ since 1800 AD (Figure 1a).

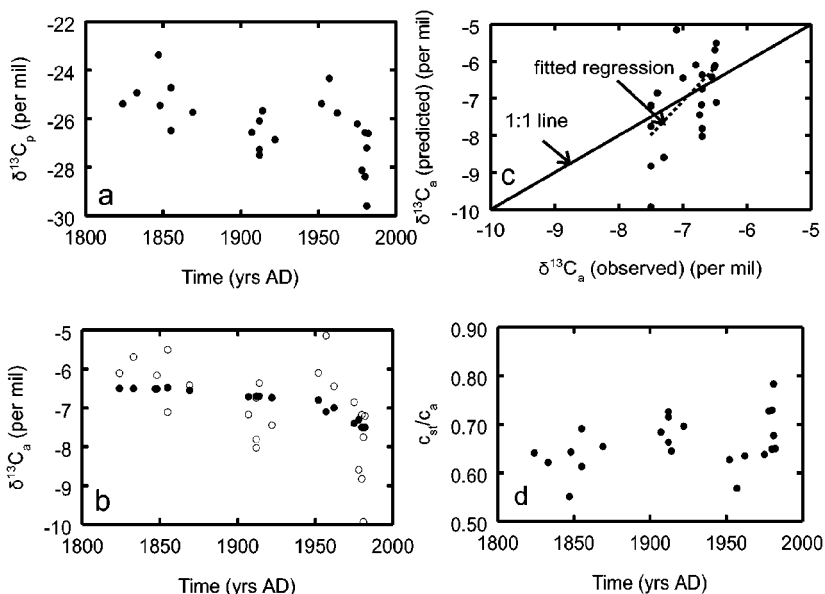


Figure 1 Historical changes in (a) the isotopic composition of herbarium tree leaves ($\delta^{13}\text{C}_p$) over the past 200 years, (b) the measured (●) and plant-derived (○) isotopic composition of atmospheric CO_2 ($\delta^{13}\text{C}_a$), (c) the correlation between predicted and measured values, and (d) calculated changes in the ratio of CO_2 partial pressures in the substomatal cavity and the atmosphere (c_{st}/c_a) from measurements of $\delta^{13}\text{C}_p$ and $\delta^{13}\text{C}_a$ (Equation 1). Data from Woodward (1993) and Beerling (1996). Plant-derived $\delta^{13}\text{C}_a$ data were calculated using measurements of $\delta^{13}\text{C}_p$ and Equation 2, as reported by Arens et al. (2000).

Over this same interval, the atmospheric $\delta^{13}\text{C}_a$ data indicate a fall of approximately 2‰ (Figure 1b) as a result of man's combustion of fossil fuels (Friedli et al. 1986). The mismatch between the two records indicates some physiological adjustment by the plants has occurred and signals trouble for Equation 2.

Using Equation 2 and the $\delta^{13}\text{C}_p$ values in Figure 1b, we calculated predicted $\delta^{13}\text{C}_a$ values for this historical sequence of leaves. The predicted $\delta^{13}\text{C}_a$ values show considerable scatter around the observations, particularly for the most recent samples. As a consequence, the approach poorly predicts $\delta^{13}\text{C}_a$ relative to the observed values (Figure 1c). The fitted regression has a slope different from unity (slope = 1.82, $r^2 = 0.34$). Constraining Equation 1 with the measurements of $\delta^{13}\text{C}_a$ and $\delta^{13}\text{C}_p$, and solving for c_{st}/c_a indicates that these trees have allowed c_{st}/c_a to increase in response CO_2 and climate change since 1950 AD (Figure 1d). The physiological adjustment violates the assumption of Arens et al. (2000) that c_{st}/c_a remains constant, leading in this case to a break down in the predictive capacity of Equation 2.

Isotopic evidence from conifer tree rings also fails to support the assumed constancy of c_{st}/c_a (Marshall & Monserud 1996, Feng 1998). Carbon isotope chronologies from natural forest conifer trees in western North America show more or less constant c_{st}/c_a ratios up until the start of the twentieth century. After this time, the response of c_{st}/c_a to CO_2 and climate becomes considerably more variable, with most of these showing a decline in c_{st}/c_a and others showing an increase. Since the work of Farquhar et al. (1982), physiologists have become increasingly aware that species vary in their discrimination against $^{13}\text{CO}_2$ and respond differently to variations in soil water, nitrogen supply, and radiation interception (Ehleringer et al. 1993). Therefore, since different species adjust their operational c_{st}/c_a values in different directions and by different magnitudes, it may be overly optimistic to expect to predict $\delta^{13}\text{C}_a$ from $\delta^{13}\text{C}_p$ with any degree of precision. These physiological considerations apply in addition to any effects of the proportional contribution of respiratory CO_2 to the source CO_2 utilized by the plants (Broadmeadow & Griffiths 1993).

Studies of herbarium leaves and tree rings provide information on the metabolic adjustment of trees to the past few hundred years of rising CO_2 levels. For paleostudies, we need information about their physiological responses on a timescale of millions of years. Therefore, we next examined the performance of Equation 2 at predicting $\delta^{13}\text{C}_a$ using $\delta^{13}\text{C}_p$ measurements made on well preserved fossil *Ginkgo adiantodes* cuticles from the early Tertiary 50 to 60 mya (Royer et al. 2001b). We used the long-term surface ocean $\delta^{13}\text{C}$ carbonate record for the same interval, with a 7‰ offset to approximate $\delta^{13}\text{C}_a$ (Veizer et al. 1999).

As with the isotopic study of historical collections of herbarium leaves, the fossil *Ginkgo* cuticles show substantial $\delta^{13}\text{C}_p$ variation of approximately 6‰ (Figure 2a) during the late Paleocene–early Eocene, which translates, via Equation 2, into large changes in $\delta^{13}\text{C}_a$ (Figure 2b). However, inferred changes in $\delta^{13}\text{C}_a$ calculated from the marine carbonates fail to show similar variations and instead record a smooth progression towards more negative values by $\sim 2\text{‰}$ – 3‰ . Consequently, there is poor correspondence between $\delta^{13}\text{C}_a$ values predicted from plant fossils and those calculated from the marine carbonate record ($r^2 = 0.02$) (Figure 2c). Solving Equation 1 for c_{st}/c_a with the measurements of $\delta^{13}\text{C}_p$ and $\delta^{13}\text{C}_a$ reconstructed from the marine carbonates indicates that the operational c_{st}/c_a ratio of *Ginkgo* has not remained constant as the global climate gradually warmed between 60 and 50 mya (Zachos et al. 2001) but instead varied between 0.55 and 0.80.

During the Paleozoic, the approach of Arens et al. (2000) could be additionally confounded by the effects of shifts in atmospheric O_2 and CO_2 composition on plant metabolic processes (Bernier et al. 2000, Beerling et al. 2002a). Theoretical models of the long-term oxygen cycle based on the sediment abundance (Bernier & Canfield 1989), and sulfur and carbon isotope mass balance budgets (Bernier et al. 2000), predict a dramatic Permo-Carboniferous $p\text{O}_2$ excursion to 35 (Figure 3). Experiments with vascular land plants have shown that growth in an O_2 -enriched atmosphere increases plant isotopic fractionation [$\Delta^{13}\text{C}$, expressed as $(\delta^{13}\text{C}_a - \delta^{13}\text{C}_p)/(1 + \delta^{13}\text{C}_p/1000)$], principally by depressing photosynthetic rates.

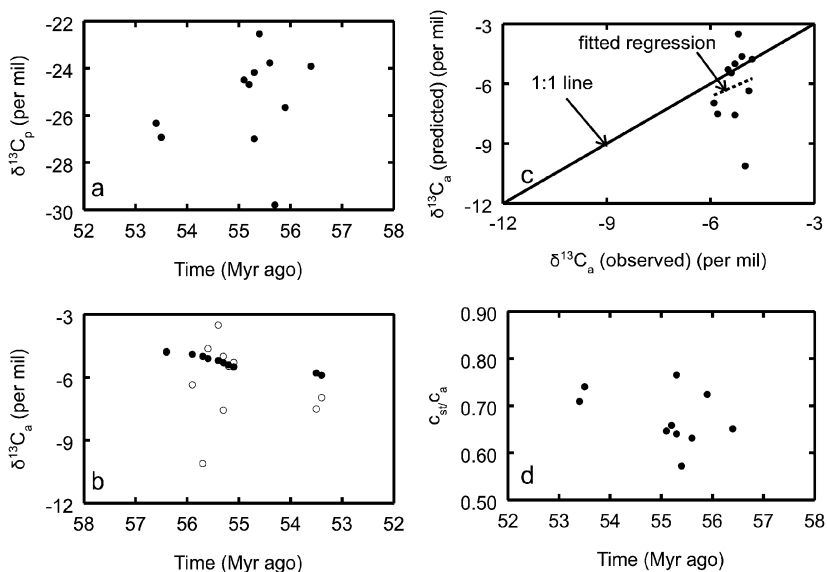


Figure 2 Changes in (a) the isotopic composition of fossil *Ginkgo* leaves ($\delta^{13}\text{C}_p$) between 58.5 and 53.4 mya, (b) the marine carbonate-derived (●) and plant-derived (○) isotopic composition of atmospheric CO_2 ($\delta^{13}\text{C}_a$), (c) the correlation between predicted and measured values, and (d) calculated changes in the ratio of CO_2 partial pressures in the substomatal cavity and the atmosphere (c_{st}/c_a) from measurements of $\delta^{13}\text{C}_p$ and reconstructed $\delta^{13}\text{C}_a$ values (Equation 1). $\delta^{13}\text{C}_p$ data from Royer et al. (2001b), $\delta^{13}\text{C}_a$ reconstructed from the global benthic carbonate compilation of Zachos et al. (2001) with a 7‰ negative offset. Plant-derived $\delta^{13}\text{C}_a$ data were calculated using measurements of $\delta^{13}\text{C}_p$ and Equation 2, as reported by Arens et al. (2000).

This lowers the photosynthetic drawdown of CO_2 in the substomatal cavity, which in turn raises c_{st}/c_a (Bernier et al. 2000, Beerling et al. 2002a).

Measurements of fossil plant $\delta^{13}\text{C}_p$ on over 50 specimens spanning the Devonian through to the Cretaceous (Beerling et al. 2002) have been used to investigate the reconstructed pattern of $\delta^{13}\text{C}_a$ using Equation 2 (Figure 3). The plant-derived $\delta^{13}\text{C}_a$ values have been compared with estimated $\delta^{13}\text{C}_a$ values based on a smoothed marine carbonate record of Veizer et al. (1999) with a 7‰ negative offset, as above. Little correspondence emerges between the plant and marine carbonate-derived $\delta^{13}\text{C}_a$ records between 400 and 350 mya. This disagreement suggests that Equation 2 is not suitable for obtaining $\delta^{13}\text{C}_a$ estimates from bulk organic matter to constrain Late Paleozoic estimates of CO_2 using the Cerling (1991, 1992) paleosol CO_2 barometer (I. Montanez et al., personal communication). The poor correspondence occurs between plant and carbonate records because of an apparent impact of the predicted Permo-Carboniferous high O_2 event on net discrimination

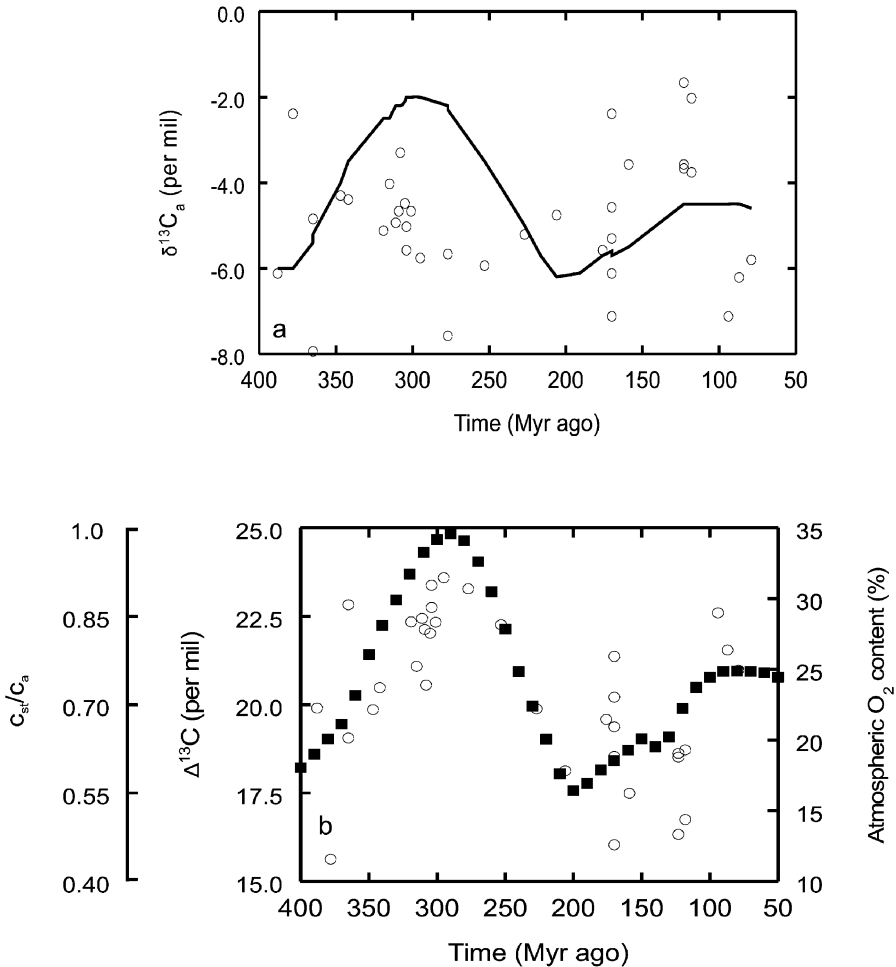


Figure 3 Comparison of changes in (a) plant-derived (○) and marine carbonate-derived (continuous line) $\delta^{13}C_a$ values between 400 and 50 mya and (b) calculated changes in carbon isotope fractionation (○), and the corresponding ratio of CO_2 partial pressures in the substomatal cavity and the atmosphere (c_{st}/c_a), and modeled fluctuations in the atmospheric O_2 content (■) (Bernier & Canfield 1989, Bernier et al. 2000). $\delta^{13}C_p$ data from Beerling et al. (2002a), $\delta^{13}C_a$ reconstructed from the global marine carbonate compilation of Veizer et al. (1999) with a 7‰ negative offset.

between plants and the atmospheric CO_2 ($\Delta^{13}C$) which reflects corresponding changes in c_{st}/c_a (Figure 3).

This section has considered at some length the potential to derive $\delta^{13}C_a$ estimates from measurements of $\delta^{13}C_p$ made on fossil plant specimens. Emphasis has been placed on testing the empirical relation produced by Arens et al. (2000) because

it may result in the generation of continuous $\delta^{13}\text{C}_a$ curves directly from terrestrial sections (Arens et al. 2000) and inferences about changes in carbon cycle processes. To better interpret these important records, it is necessary to rigorously evaluate the technique before it passes into common usage. The approach however has failed the two different tests applied here because it assumes plants maintain c_{st}/c_a at a constant value in the long- and short-term.

Mechanistic biochemical models of CO_2 uptake by leaves of C_3 plants are available (Farquhar et al. 1980) and can be coupled with models of empirical stomatal responses to the environment (e.g., Leuning 1995). A more robust approach to estimating $\delta^{13}\text{C}_a$ from fossil plants when needed, therefore, might be to estimate the equilibrium solution value of c_{st}/c_a using the necessary paleoenvironmental information. This environment-constrained c_{st}/c_a value might then be used to solve Equation 1 for $\delta^{13}\text{C}_a$. Even this approach will fail to account for species-specific differences in $^{13}\text{CO}_2$ discrimination but it would place paleo- $\delta^{13}\text{C}_a$ estimates on a more mechanistic basis.

STOMATAL INDEX AS A PALEO- CO_2 PROXY

There is a strong selective pressure in vascular land plants to minimize water loss through their stomatal pores during photosynthetic CO_2 uptake and the attendant risks of lethal dehydration. To achieve this, plants regulate leaf gas exchange so as to maximize carbon fixation per unit of water loss per unit of time (i.e., water-use efficiency, WUE). Stomata-bearing plants partially control transpirational water loss and WUE by altering pore widths and, under some circumstances, their stomatal numbers. If, for example, the concentration of atmospheric CO_2 increases, then plants can reduce their stomatal pore area without loss of photosynthetic productivity. This response in turn decreases leaf water loss, increasing the WUE of growth. Woodward (1987) first documented from herbaria collections of leaves a reduction in both stomatal density (SD, stomata per unit area) and stomatal index (SI, percentage of epidermal cells that are stomata) in the leaves of eight temperate woody species in response to the anthropogenic rise in CO_2 over the past 200 years. This inverse response to CO_2 increases has been observed in over 60 other species and reproduced in experiments (see Woodward & Kelly 1995 and Royer 2001 for reviews). Stomata in most C_3 plants are therefore sensitive indicators of CO_2 change, at least within the range of 280–370 ppmv. This stomatal relationship can be readily inverted and applied to the fossil record as a CO_2 proxy for both reconstructing paleo- CO_2 change and gaining insight into the fluxes among the carbon cycle reservoirs.

Constraints on the Method

STOMATAL INDEX YIELDS A MORE RELIABLE SIGNAL Experimental studies and observations on natural plant communities indicate that stomatal density is influenced by the water potential gradients within leaves and within canopies (including

sun versus shade leaves), whereas stomatal index is largely independent of these factors (see Beerling 1999 and Royer 2001 for overviews). Water stress appears to affect epidermal cell size (and thus SD) but not stomatal initiation rates (and thus SI). Light intensity, however, often affects both SD and SI and is most pronounced when the irradiance treatments are applied during the period of leaf development (Schoch et al. 1980, Lake et al. 2001). During other periods of plant growth, irradiance only affects epidermal cell size (and thus SD) through the conflating effect of water stress.

Stomatal index is therefore influenced by fewer environmental factors (in addition to CO₂), and should yield a more reliable signal of CO₂ change (Beerling 1999, Royer 2001). When possible, then, SI (or another comparable area-independent parameter) should always be measured.

SPECIES-SPECIFIC NATURE Although the SI (and SD) in most plants is sensitive to CO₂, inter-specific relationships usually vary. Woodward & Kelly (1995) found no taxonomic dependency in SD based on an analysis of 100 species, reporting that even intrageneric responses display marked variability. For example, for genera represented by >1 species in the compilation of Royer (2001), only 3 (19%) and 1 (14%) responded in a consistent fashion to CO₂ for SD and SI, respectively. Unless it can be demonstrated otherwise, one must assume that the stomatal responses to CO₂ are species specific. This means that only single species or morphotypes can be tracked in the fossil record, and these data must be compared to the same species in the modern record.

NONLINEAR RESPONSE AT ELEVATED CO₂ The inverse responses of SI to CO₂ between subambient and present-day concentrations (~340–350 ppmv) are typically linear. In most plants, however, SI shows a reduced sensitivity at elevated CO₂, resulting in a nonlinear response from subambient to elevated CO₂ levels (Beerling 1999, Beerling & Royer 2002). Royer et al. (2001b) documented this type of response in two deciduous gymnosperms, *Ginkgo biloba* and *Metasequoia glyptostroboides* (Figure 4).

It has been suggested previously that the source of this nonlinearity is the extended period of time that modern lineages experienced subambient CO₂ levels [at least 420,000 years (Petit et al. 1999)], which in turn has dampened the phenotypic response in stomata at high CO₂ (Beerling & Chaloner 1993, Woodward & Bazzaz 1988, Royer 2001, Beerling & Royer 2002). Implicit in this argument is that given sufficient exposure time to elevated CO₂, stomata will respond. Beerling & Royer (2002) tested this assumption by independently calibrating a set of SI measurements from fossil *Ginkgo* cuticles ranging in age from 56.5 to 53.5 mya with coeval pedogenic carbonate-derived paleo-CO₂ estimates. Such long time-scales presumably represent sufficient time for plants to adapt. Both the fossil cuticles and carbonates came from the same field area (Bighorn Basin, Wyoming and Montana, U.S.A.), and the $\delta^{13}\text{C}$ values from the *Ginkgo* cuticles were used to constrain the organic matter $\delta^{13}\text{C}$ values required for reconstructing CO₂ from

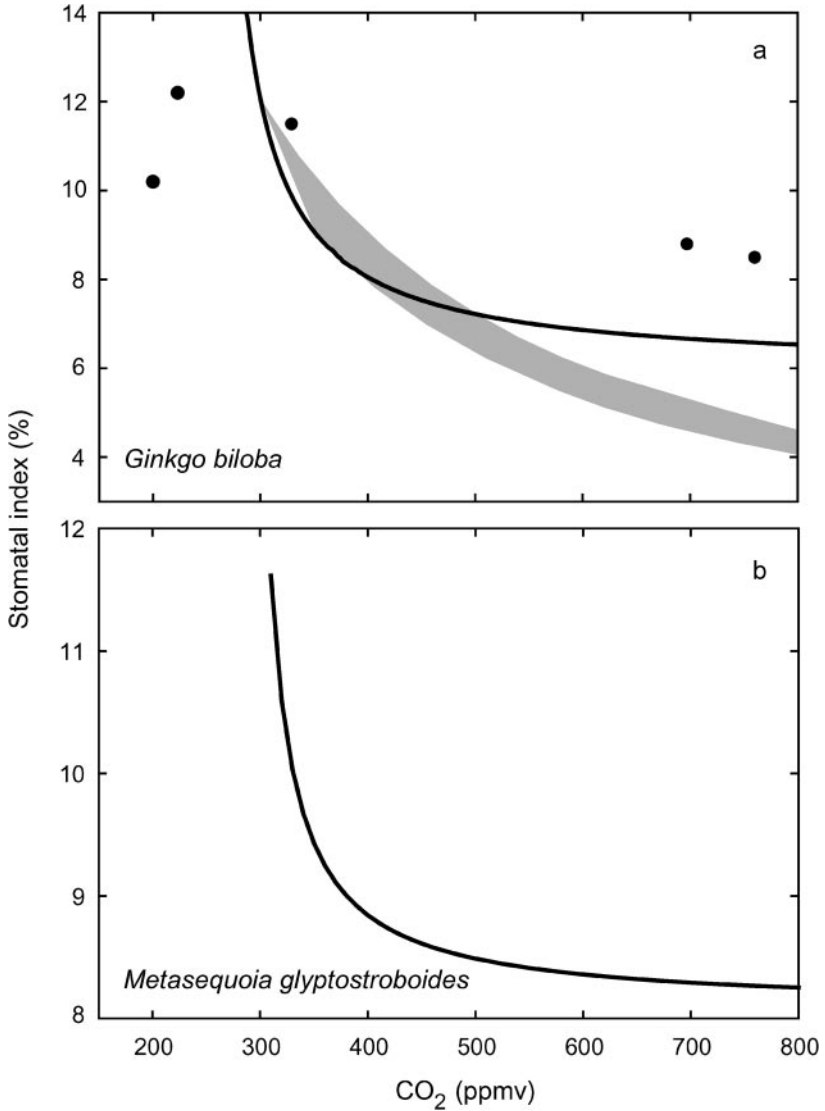


Figure 4 Response of leaf stomatal index of (a) *Ginkgo biloba* and (b) *Metasequoia glyptostroboides* to a wide range of atmospheric CO₂ levels. Lines represent regressions [*Ginkgo*: $r^2 = 0.91$, $F(1,38) = 195$, $P < 0.001$; *Metasequoia*: $r^2 = 0.85$, $F(1,16) = 41$, $P < 0.001$] derived from herbaria sheets and CO₂-controlled greenhouses. SI-CO₂ calibration derived from fossil cuticles and coeval pedogenic carbonate paleo-CO₂ estimates (●) is shown for *Ginkgo*. Stomatal ratio calibration is also shown for *Ginkgo* (shaded region), where the range in CO₂ was generated using leaves that developed in either a 300 ppmv (SI = 12.1%) or 350 ppmv (SI = 9.1%) atmospheric CO₂ concentration.

the pedogenic carbonates (Cerling 1991, Ekart et al. 1999). Although the error margins associated with this CO₂ proxy are comparatively large (± 300 ppmv), the carbonate-derived SI-CO₂ training set is remarkably similar to the modern training set derived from herbaria material and leaves from CO₂-controlled greenhouses (Figure 4). This analysis supports the use of largely phenotypic responses inherent in experiments and herbaria leaves for calibrating the genotypic responses dominant in multi-million year fossil sequences because it suggests that the structure in both are similar. Unfortunately, however, it further indicates that the SI technique loses sensitivity at high CO₂, and, in the case of *Ginkgo*, is probably not appropriate for quantitatively reconstructing CO₂ concentrations exceeding ~ 500 ppmv.

Although most species lose much of their sensitivity at high CO₂, groups of evolving plants appear to continue to respond even at very high CO₂ levels. Beerling & Woodward (1997) and Royer (2001) compiled pre-Quaternary records of the SD and SI of fossil leaves, and reported high values during the Late Paleozoic and Late Cenozoic when atmospheric CO₂ concentrations calculated from geochemical carbon cycle models (Berner & Kothavala 2001) and other CO₂ proxies (see compilation in Crowley & Berner 2001) are low. Conversely, uniformly low stomatal densities were evident throughout the remainder of the record when atmospheric CO₂ levels were high. Carrying this pattern further, McElwain (1998) (McElwain & Chaloner 1995, 1996) compared fossil SI measurements with their respective extant ecological and morphological equivalents [nearest living equivalents (NLE)]. By directly converting the stomatal ratio (SR) of the modern equivalent to the fossil material into a paleo-CO₂ estimate such that a SR of 2 equates to a CO₂ estimate of 700 ppmv (assuming the leaves from the modern material developed in a 350 ppmv atmosphere), McElwain (1998) found that SR-derived estimates correlated well with the model-derived CO₂ predictions of Berner (1994) (Berner & Kothavala 2001). The method is nonquantitative because it assumes, a priori, a prescribed nonlinear relationship between SI_{fossil} and CO₂, such that SI_{fossil} $\propto 1/\text{CO}_2$. However, in the case of *Ginkgo*, the SR-derived calibration curve matches the training set-derived estimates reasonably well, lending support to this approach (Beerling & Royer 2002; see Figure 4). The principal advantage of this method, in contrast to the training set-derived approach, is that it is taxonomically independent and thus can be applied back to the Devonian (400 mya; McElwain & Chaloner 1995).

SAMPLE SIZE It is important to measure SI on a sufficient number of leaves to account for the natural variability of the population (Poole & Kürschner 1999). For example, Figure 5 shows the sensitivity of the cumulative mean of SI in *Ginkgo adiantoides* to the number of cuticle fragments measured for four latest Cretaceous to early Eocene sites. In all cases, counts were made on three intercostal (between veins) fields of view per cuticle fragment. Such plots are useful for determining the minimum number of leaves required for accurate SI results (Poole & Kürschner 1999). For *G. adiantoides*, these plots indicate that ≥ 5 leaves should be

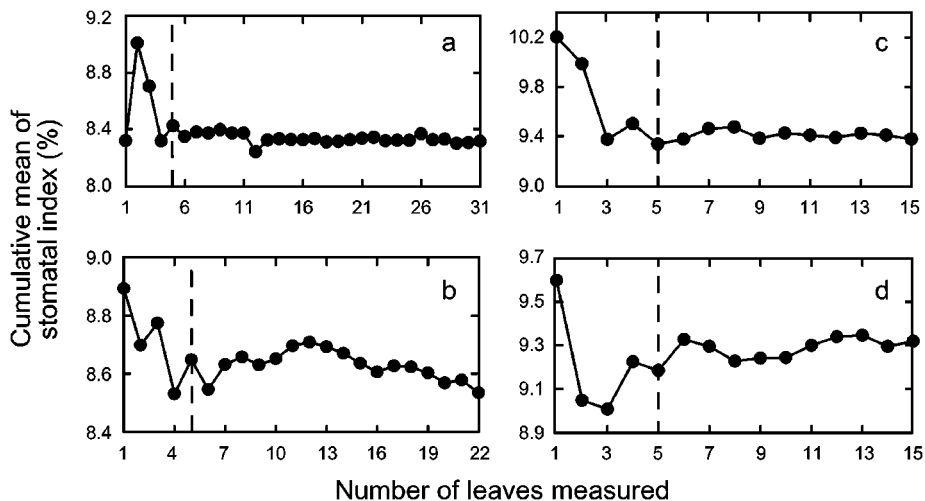


Figure 5 Sensitivity of the cumulative mean of SI in *Ginkgo adiantoides* to the number of cuticle fragments measured. The dashed lines highlight the cumulative means based on five fragments. The four fossil sites are: (a) DMNH 566, Hell Creek Formation, North Dakota (U.S.A.); (b) SLW 9812, Willwood Formation, Wyoming (U.S.A.); (c) LJH 9915, Willwood Formation, Wyoming (U.S.A.); and (d) LJH 7659, Fort Union Formation, Wyoming (U.S.A.).

sampled before being used for paleo- CO_2 reconstructions. In normally distributed samples, the measurement of five leaves translates to a 95% confidence interval of $\pm 0.88 \times \sigma$, where σ is the standard deviation of the sample.

Both Retallack (2001) and Royer et al. (2001b) reconstructed paleo- CO_2 levels from *Ginkgo* cuticles, but the studies differed in the number of leaves used to obtain a mean SI for a given time interval (Figure 6). Frequency histograms of the number of leaves measured per site for both studies reveal that approximately half of the CO_2 estimates reconstructed by Retallack (2001) were based on fewer than five cuticle fragments (Figure 6). This limited replication introduces a significant degree of imprecision into the CO_2 estimates and may help explain why no discernable patterns emerged from the 300 Ma record of fossil plant cuticles. Other studies with ancient *Ginkgo*-type taxa (e.g., Chen et al. 2001) that obtained secure SI measurements based on well-replicated counts found patterns of CO_2 change for the Mesozoic consistent with that calculated from long-term carbon cycle models (Berner & Kothavala 2001).

Case Studies

EARLY TERTIARY CO_2 Atmospheric CO_2 is an important greenhouse gas. It is crucial, therefore, to estimate past CO_2 concentrations if we are to understand its role in regulating global climate, particularly during periods of extreme global warmth.

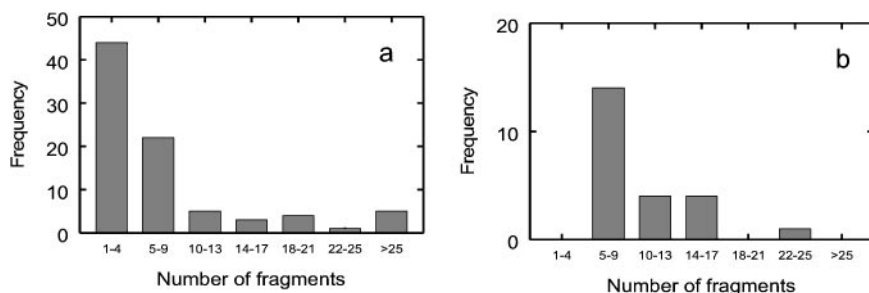


Figure 6 Frequency histogram of the number of *Ginkgo* cuticle fragments measured per CO₂ estimate for the study of (a) Retallack (2001), and (b) Royer et al. (2001b). Only those collections deemed statistically adequate in the study of Retallack (2001) are included here.

The early Tertiary (Paleocene to Middle Eocene, 65–45 mya) represents such an interval, with marine sediment cores indicating ocean bottom waters 8°C–12°C warmer than the present-day (Zachos et al. 2001) and high latitude sea surface temperatures upwards of 15°C warmer (Zachos et al. 1994). Unfortunately, estimates of CO₂ for this interval vary widely: <300 to 2000 ppmv using pedogenic carbonates (Ekart et al. 1999, Royer et al. 2001b), 300–1000 ppmv using geochemical models (Berner & Kothavala 2001), and 500–3500 ppmv using boron isotopes in marine carbonates (Pearson & Palmer 2000).

Because of this uncertainty, a recent study focused on estimating CO₂ levels for the same period using the stomatal approach. Royer et al. (2001b) measured the stomatal indices of *G. adiantoides* from a series of 19 well-dated North American and one northern European fossil plant sites spanning in age from 58.5 to 53.4 mya. Modern *G. biloba* is unusual among vascular land plants in having an extremely long fossil record, and is considered conspecific with its fossil equivalent, *G. adiantoides*, by several paleobotanists (Tralau 1968). This affords the rare opportunity to directly calibrate early Tertiary measurements of SI to a training set derived from modern plants. Following this procedure, Royer et al. (2001b) found that all reconstructed CO₂ values fell between 300 and 450 ppmv with the exception of one high value near the P/E boundary (Figure 7). If correct, explanation of the globally warm temperatures during this interval requires a consideration of climate forcing factors in addition to CO₂ (e.g., paleogeography, clouds, vegetative feedbacks).

The site corresponding with the one high CO₂ estimate (Figure 7) may date to the P/E boundary. The distinctive carbon isotope excursion was not observed at this site (Royer et al. 2001b), and, in addition, is the one non-North American site in the dataset (Arduin Head, Isle of Mull, Scotland, U.K.) and is based on cuticles of *G. gardneri*, not *G. adiantoides*. Nevertheless, a positive CO₂ excursion has not been reproduced using other CO₂ proxies across this event, an excursion that is

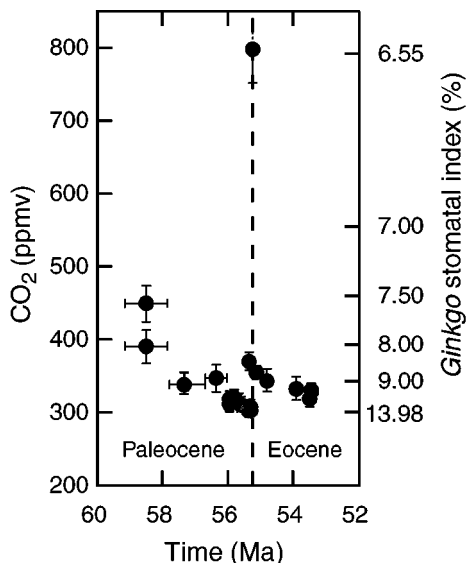


Figure 7 Reconstruction of paleo-CO₂ for the middle Paleocene to early Eocene based on SI measurements from *Ginkgo* fossil cuticles. Errors represent $\pm 95\%$ confidence intervals. Adapted from Royer et al. (2001b).

required if the methane hypothesis is correct, and so further stratigraphic work is certainly warranted at Ardtun Head.

A MESOZOIC CO₂ RECONSTRUCTION FROM STOMATAL RATIOS OF GINKGO

The earliest remains of *G. adiantoides* date to the Early Cretaceous, but they do not become abundant until the Late Cretaceous (Tralau 1968). Given that few monospecific lineages extend from the present-day back to the pre-Cretaceous, an alternative method must be used to reconstruct pre-Cretaceous CO₂ concentrations from stomata. The stomatal ratio method, introduced above, compares the SI of a fossil species to its NLE, and then directly translates this stomatal ratio into a semiquantitative estimate of atmospheric CO₂.

Remains of the genus *Ginkgo* extend back to the late Triassic, and many SI measurements from Mesozoic *Ginkgo* cuticles have been made in recent years (Beerling et al. 1998, McElwain et al. 1999, Chen et al. 2001, Retallack 2001). By comparing the SIs of its NLE (*G. biloba*) grown in a 300 ppmv atmosphere [RCO₂; corresponding SI = 12.1% (Royer et al. 2001b)] to the fossils ($n = 20$ sites), we reconstructed CO₂ in a semiquantitative fashion (Figure 8; Table 1).

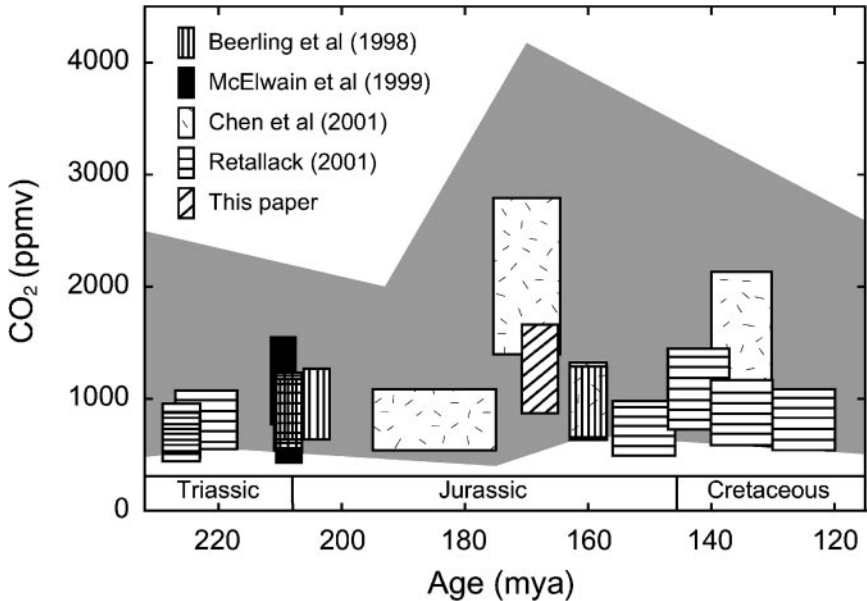


Figure 8 A stomatal-derived CO₂ reconstruction based on a compilation of SI measurements of Mesozoic *Ginkgo* (see Table 1 for raw data). CO₂ estimated using the semiquantitative stomatal ratio technique. The error range in CO₂ for each estimate was generated by comparing calculations assuming 1 SR = 1 RCO₂ (such that CO₂ = SR × 300 ppmv; e.g., McElwain 1998) with 1 SR = 2 RCO₂ (such that CO₂ = SR × 600 ppmv; e.g., McElwain et al. 1999). The shaded region corresponds to the range of CO₂ predictions from the geochemical carbon cycle model of Berner & Kothavala (2001).

Most of the stomatal estimates of Mesozoic atmospheric CO₂ levels lie between 1000 and 2000 ppmv (Figure 8). This range fits within the lower bounds of the geochemical model-derived CO₂ predictions (Figure 8), and is in broad agreement with pedogenic carbonate-derived CO₂ estimates, which range from 1000–5000 ppmv (Ekart et al. 1999, Ghosh et al. 2001). These results support the plausibility of a CO₂-forced greenhouse during this globally warm interval (Crowley & Berner 2001).

FUTURE DIRECTIONS

Carbon Isotopes

MOLECULES AND MODELS Ongoing developments in mass spectrometry allow increasingly smaller sample sizes to be measured (down to ng). Using a gas chromatograph coupled to a mass spectrometer, for instance, isotopic measurements can be made on individual compounds (Hinrichs et al. 2001). These advances

TABLE 1 Measurements of stomatal index from Mesozoic *Ginkgo* cuticles

Study	Species	Period	Age ^a (mya)	Stomatal index (%)
Beerling et al. (1998)	<i>Ginkgoites</i> ^b <i>troedssonii</i>	Late Triassic (Rhaetian)	209	5.9
	<i>Ginkgoites marginata</i>	Late Triassic (Rhaetian)	209	6.5
	<i>Ginkgoites marginata</i>	Early Jurassic (Hettangian)	204	5.7
	<i>Ginkgo huttoni</i>	Middle Jurassic	160	5.6
McElwain et al. (1999)	<i>Ginkgoites obovatus</i>	Late Triassic (Rhaetian)	210	4.7
	<i>Ginkgoites obovatus</i>	Late Triassic (Rhaetian)	209	6.8
	<i>Ginkgoites acosmica</i>	Late Triassic (Rhaetian)	209	8.5
Chen et al. (2001)	<i>Ginkgo obrutschewii</i>	Early Jurassic	185	6.7
	<i>Ginkgo yimaensis</i>	Middle Jurassic	170	2.6
	<i>Ginkgo huttoni</i>	Middle Jurassic	160	5.5
	<i>Ginkgo coriacea</i>	Early Cretaceous (Valanginian-Hauterivian)	135	3.4
Retallack (2001) ^c	<i>Ginkgo matatiensis</i>	Late Triassic (Carnian)	226	8.2
	<i>Ginkgo telemachus</i>	Late Triassic (Carnian)	226	7.6
	<i>Ginkgoites lunzensis</i>	Late Triassic (Carnian)	222	6.7
	<i>Ginkgoites troedssonii</i>	Late Triassic (Rhaetian)	209	6.0
	<i>Ginkgo manchurica</i>	Late Jurassic (Kimmeridgian-Tithonian)	151	7.4
	<i>Ginkgo manchurica</i>	Early Cretaceous (Berriasian)	140	5.0
	<i>Ginkgo coriacea</i>	Early Cretaceous (Valanginian-Hauterivian)	135	6.2
	<i>Ginkgo polaris</i>	Early Cretaceous (Barremian)	125	6.7
This paper	<i>Ginkgo dahlii</i>	Middle Jurassic	168	4.5

^a From Harland et al. (1989).

^b *Ginkgoites* is considered a synonym of *Ginkgo* by Cziesler (1998).

^c Only measurements based on ≥ 5 cuticle fragments are included here (see text).

mean that it is possible to analyze the isotopic composition of specific compounds isolated from bulk organic matter and, by appropriate selection of compounds, separate marine and terrestrial isotopic signals (e.g., Kuypers et al. 1999). The study of molecular fossils, therefore, has the potential to retrieve information on carbon exchange and burial rates from bulk sediment samples that allows much improved analyses of ancient carbon cycle processes. The future application of these techniques to intervals of abrupt climatic change and mass extinction represents a promising area of future research (Crowley & North 1988).

A further promising, but under exploited, area of research utilizing plant $\delta^{13}\text{C}$ data is the use of paleoclimate simulations to drive process-based representations of terrestrial ecosystem carbon cycling, and the associated fractionation of carbon isotopes. A better understanding of the isotopic fractionations occurring during photosynthesis (Farquhar & Lloyd 1993, Lloyd & Farquhar 1994) and soil organic

matter cycling by land plants (Ciais et al. 1999) allows simulation of the $\delta^{13}\text{C}$ of above- and below-ground terrestrial organic matter using only climate information generated by computer models. Comparison of model predictions with $\delta^{13}\text{C}$ measurements and calculated fractionation values from fossil plant materials offers a new means of evaluating global paleoclimates. This approach has the advantage of being based on a mechanistic understanding of the processes involved, integrating climate model seasonal cycles of near-surface temperature, precipitation, and atmospheric moisture, and has the capacity to predict $\delta^{13}\text{C}_p$ at local or regional scales. Moreover, it would allow evaluation of global paleoclimate simulations without resorting to correlations between climate and vegetation type (or biome) (e.g., Rees et al. 1999)—an approach probably flawed at times of higher-than-present atmospheric CO_2 levels (Beerling 1998).

Stomata

To date, few studies have quantitatively reconstructed CO_2 by calibrating the SIs of a monospecific sequence of fossil leaves to a modern training set of the same species. These include studies from the Holocene (Rundgren & Beerling 1999, Wagner et al. 1999), Late Miocene and Pliocene (van der Burgh et al. 1993, Kürschner et al. 1996), and latest Cretaceous to Early Eocene (Royer et al. 2001b). Clearly, there are other long-ranging species that can be exploited to further develop a more complete stomata-based CO_2 reconstruction for the Cenozoic. One target area should be the Late Eocene to Oligocene (39 to 23 mya) because of the general dearth of CO_2 estimates (for all proxies, in fact) during this interval (e.g., Royer et al. 2001a). Given the large inconsistencies among the various CO_2 proxies for the early Tertiary (65 to 50 mya, see above), this interval should also be targeted for further stomatal research. On a more general note, southern hemisphere stomata-based reconstructions are required to provide a cross-check on the strictly northern hemisphere reconstructions published thus far.

One clear advantage of the stomatal method over most other CO_2 proxies is that the SI of leaves responds to CO_2 change in <1 year. It is therefore ideal for discerning rapid excursions (Royer et al. 2001a). This approach has proven successful for the T/J boundary (McElwain et al. 1999), the early Holocene (Wagner et al. 1999), and possibly the P/E boundary (Royer et al. 2001a, see above). The geologic record probably contains numerous other short-term CO_2 events, including the K/T boundary, and methane hydrate events (e.g., Permian/Triassic boundary: Krull & Retallack 2000; Early Jurassic: Hesselbo et al. 2000; Late Jurassic: Padden et al. 2001; Early Cretaceous: Jahren et al. 2001).

PALEOELEVATION Stomata respond to changes in CO_2 partial pressure, not mole fraction (Woodward 1986, Woodward & Bazzaz 1988). One consequence of this characteristic is that the SD and SI in many plants increase with elevation (Körner & Cochrane 1985, Woodward 1986). This potential source of variability should be controlled, or corrected, for in fossil studies aiming to reconstruct paleo- CO_2

concentrations. For example, Royer et al. (2001b) selected fossil sites with paleoelevations at or near sea-level, where gas partial pressure \cong concentration.

The confounding factor of elevation, however, can in theory be turned around and used as a predictive variable. In this case, where paleoelevation is being calculated, CO₂ concentration must be controlled for. An ideal setting for applying this approach would be to compare an autochthonous fossil-bearing sequence with intertonguing marine or tidal sediments (and thus near sea-level) with a nearby, isochronous and autochthonous fossil-bearing sequence of unknown paleoelevation. By quantifying the difference in SI between the two sites, paleoelevation could be extracted. Alternatively, the difference in paleoelevation between two non-sea-level isochronous sites could also be calculated. This type of application may be useful for constraining mountain uplift rates.

Elevation can be calculated from CO₂ partial pressure in the following manner (derived from Jones 1992):

$$elev(p_2) = -\ln\left(\frac{p_2}{p_1}\right) \times \frac{\mathfrak{R} \times T}{(M_A \times g)}, \quad (3)$$

where p_1 and p_2 are the CO₂ partial pressures (Pa) at sea-level and the unknown site, respectively, \mathfrak{R} is the gas constant (8.3144 Pa m³ mol⁻¹ K⁻¹), T is the mean temperature (K) of the range in elevation, M_A is the molecular weight of air (0.028964 kg mol⁻¹), g is the acceleration due to gravity (9.8 m s⁻²), and $elev_{p_2}$ is the elevation (m) of the unknown site. p_2/p_1 can be closely approximated by calculating the ratio of the two CO₂ concentrations (ppmv) derived from stomatal indices, such that a sea-level estimate of 600 ppmv and a value of 400 ppmv at an isochronous site of unknown elevation yields a p_2/p_1 of 0.67, and a paleoelevation estimate of 3350 m. Temperature effects are minor. For example, raising the mean temperature from 10°C to 30°C increases elevation estimates by <10%. This technique is admittedly crude, as it depends both on well-constrained sedimentary settings and the sensitivity of stomatal indices to changes in CO₂ partial pressure.

As a preliminary example, we calculated the possible range of paleoelevation that could be estimated using Equation 3 and the relationship between SI and CO₂ in *Ginkgo* reported by Royer et al. (2001b). It emerges that a wide range of paleoelevation could be extracted from *Ginkgo* (up to ~3000 m), particularly if sea-level CO₂ partial pressure was high (40 Pa, or ~400 ppmv). The potential for reasonably precise estimates is high, particularly at high paleoelevations/high stomatal indices (Figure 9). In general, most SI estimates for a given site are precise ($\pm 95\%$ confidence interval), within ± 0.5 units, or a total of 1 SI unit. Figure 9 provides a rough gauge for the estimation of measurement-derived error. In the case of *Ginkgo*, this error is always less than ± 500 m. Other currently used paleoelevation indicators are, on average, less precise. For example, paleobotanical indicators that rely on changes in vegetation assemblages (Axelrod 1997) or leaf physiognomy (Gregory & Chase 1992, Wolfe et al. 1997) are usually associated with error margins of more than ± 1000 m. In areas of good stratigraphic control, stomata, by virtue of their response to past CO₂ levels, appear to be very promising atmospheric barometers.

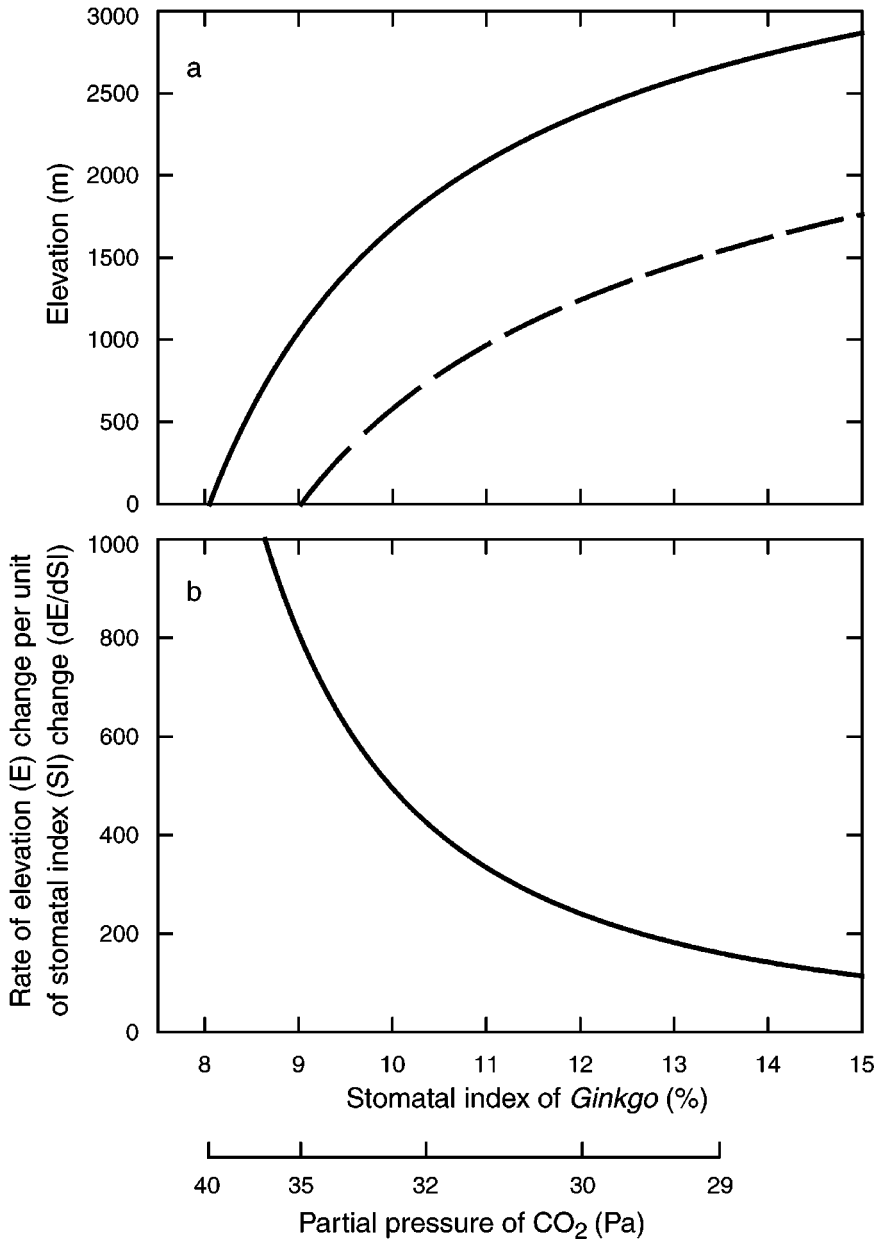


Figure 9 (a) Predictions of elevation based on the SI-CO₂ relationship reported by Royer et al. (2001b). The two curves represent predictions anchored with sea-level CO₂ partial pressures of 35 Pa (*dashed line*) and 40 Pa (*solid line*). (b) The first differential of the curves in (a).

ACKNOWLEDGMENTS

We thank R.A. Berner and C.P. Osborne for helpful reviews and comments, and József Pálffy for sight of his in press manuscript. DJB gratefully acknowledges funding through a Royal Society University Research Fellowship and the Leverhulme Trust, and DLR acknowledges an NSF Graduate Research Fellowship.

Visit the Annual Reviews home page at www.annualreviews.org

LITERATURE CITED

- Algeo TJ, Scheckler SE. 1998. Terrestrial-marine teleconnections in the Devonian: links between the evolution of land plants, weathering processes, and marine anoxic events. *Philos. Trans. R. Soc. London Ser. B* 353: 113–30
- Arens NC, Jahren AH. 2000. Carbon isotope excursion in atmospheric CO₂ at the Cretaceous-Tertiary boundary: evidence from terrestrial sediments. *Palaios* 15:314–22
- Arens NC, Jahren AH, Amundson R. 2000. Can C₃ plants faithfully record the carbon isotopic composition of atmospheric carbon dioxide? *Paleobiology* 26:137–64
- Arinobu T, Ishiwatari R, Kaiho K, Lamolda MA. 1999. Spike of pyrosynthetic polycyclic aromatic hydrocarbons associated with an abrupt decrease in $\delta^{13}\text{C}$ of a terrestrial biomarker at the Cretaceous-Tertiary boundary at Caravaca, Spain. *Geology* 27:723–26
- Axelrod DI. 1997. Paleoelevation estimated from Tertiary Floras. *Int. Geol. Rev.* 39: 1124–33
- Beerling DJ. 1996. Ecophysiological responses of woody plants to past CO₂ concentrations. *Tree Physiol.* 16:389–96
- Beerling DJ. 1997. Interpreting environmental and biological signals from the stable carbon isotope composition of fossilized organic and inorganic carbon. *J. Geol. Soc. London* 154:303–9
- Beerling DJ. 1998. The future as the key to the past for palaeobotany? *Trends Ecol. Evol.* 13:311–16
- Beerling DJ. 1999. Stomatal density and index: theory and application. See Jones & Rowe 1999, pp. 251–56
- Beerling DJ. 2000. Global terrestrial productivity in the Mesozoic era. In *Climates: Past and Present*, ed. MB Hart, pp. 17–32. London: Geol. Soc. 218 pp.
- Beerling DJ. 2002. Palaeo-CO₂ changes during the end-Triassic mass extinction. *Nature*. 415:386–87
- Beerling DJ, Chaloner WG. 1993. Evolutionary responses of stomatal density to global CO₂ change. *Biol. J. Linn. Soc.* 48:343–53
- Beerling DJ, Jolley DW. 1998. Fossil plants record an atmospheric ¹²CO₂ and temperature spike across the Palaeocene-Eocene transition in NW Europe. *J. Geol. Soc. London* 155:591–94
- Beerling DJ, Lake JA, Berner RA, Hickey LJ, Taylor DW, Royer DR. 2002a. Isotopic evidence for a Permo-Carboniferous high-oxygen event. *Geochem. Cosmochim. Acta*. In press
- Beerling DJ, Lomas MR, Grocke DR. 2002b. On the nature of methane gas-hydrate dissociation during the Toarcian and Aptian oceanic anoxic events. *Am. J. Sci.* In press
- Beerling DJ, Lomax BH, Upchurch GR, Nichols DJ, Pillmore CL. 2001. Evidence for the recovery of terrestrial ecosystems ahead of marine primary production following a biotic crisis at the Cretaceous-Tertiary boundary. *J. Geol. Soc. London*. 158:737–40
- Beerling DJ, McElwain JC, Osborne CP. 1998. Stomatal responses of the 'living fossil' *Ginkgo biloba* L. to changes in atmospheric CO₂ concentrations. *J. Exp. Bot.* 49:1603–7

- Beerling DJ, Royer DL. 2002. Reading a CO₂ signal from fossil stomata. *New Phytol.* In press
- Beerling DJ, Woodward FI. 1997. Changes in land plant function over the Phanerozoic: reconstructions based on the fossil record. *Bot. J. Linn. Soc.* 124:137–53
- Berner RA. 1994. GEOCARB II: A revised model of atmospheric CO₂ over Phanerozoic time. *Am. J. Sci.* 294:56–91
- Berner RA. 1997. The rise of plants and their effect on weathering and atmospheric CO₂. *Science* 276:544–6
- Berner RA. 1998. The carbon cycle and CO₂ over Phanerozoic time: The role of land plants. *Philos. Trans. R. Soc. London Ser. B* 353:75–82
- Berner RA, Caufield DE. 1989. A new model for atmospheric oxygen over Phanerozoic time. *Am. J. Sci.* 289:59–91
- Berner RA, Kothavala Z. 2001. GEOCARB III: a revised model of atmospheric CO₂ over Phanerozoic time. *Am. J. Sci.* 301:182–204
- Berner RA, Petsch ST, Lake JA, Beerling DJ, Popp BN, et al. 2000. Isotope fractionation and atmospheric oxygen: implications for Phanerozoic O₂ evolution. *Science* 287:1630–33
- Berninger F, Sonninen E, Aalto T, Lloyd J. 2000. Modeling ¹³C discrimination in tree rings. *Global Biogeochem. Cycles* 14:213–23
- Broadmeadow MSJ, Griffiths H. 1993. Carbon isotope discrimination and the coupling of CO₂ fluxes within forest canopies. See Ehleringer et al. 1993, pp. 109–29
- Broecker WS, Peacock S. 1999. An ecologic explanation for the Permo-Triassic carbon and sulfur isotope shifts. *Global. Biogeochem. Cycles* 13:1167–72
- Cerling TE. 1991. Carbon dioxide in the atmosphere: evidence from Cenozoic and Mesozoic paleosols. *Am. J. Sci.* 291:377–400
- Cerling TE. 1992. Use of carbon isotopes in paleosols as an indicator of the P(CO₂) of the paleoatmosphere. *Glob. Biogeochem. Cycles* 6:307–14
- Chen L-Q, Li C-S, Chaloner WG, Beerling DJ, Sun Q-G, et al. 2001. Assessing the potential for the stomatal characters of extant and fossil *Ginkgo* leaves to signal atmospheric CO₂ change. *Am. J. Bot.* 88:1309–15
- Ciais P, Denning AS, Tans PB, Berry JA, Randall DA, et al. 1997. A three-dimensional synthesis study of δ¹⁸O in atmospheric CO₂. 1. Surface fluxes. *J. Geophys. Res.* D102:5857–72
- Ciais P, Friedlingstein P, Schimel DS, Tans PP. 1999. A global calculation of the δ¹³C of soil respired carbon: implications for the biospheric uptake of anthropogenic CO₂. *Global Biogeochem. Cycles* 13:519–30
- Crowley TJ, Berner RA. 2001. CO₂ and climate change. *Science* 292:870–2
- Crowley TJ, North GR. 1988. Abrupt climate change and extinction events in Earth history. *Science* 240:996–1002
- Czier Z. 1998. *Ginkgo* foliage from the Jurassic of the Carpathian Basin. *Palaeontology* 41:349–81
- DeNiro MJ, Epstein S. 1978. Influence of diet on the distribution of carbon isotopes in animals. *Geochim. Cosmochim. Acta* 42:495–506
- D'Hondt S, Donaghay P, Zachos JC, Luttenberg D, Lindinger M. 1998. Organic carbon fluxes and ecological recovery from Cretaceous-Tertiary mass extinction. *Science* 282:276–79
- Dickens GR, Castillo MM, Walker JCG. 1997. A blast of gas in the latest Paleocene: simulating first-order effects of massive dissociation of oceanic methane hydrate. *Geology* 25:259–62
- Dickens GR, O'Neil JR, Rea DK, Owen RM. 1995. Dissociation of oceanic methane hydrate as a cause of the carbon isotope excursion at the end of the Paleocene. *Paleoceanography* 10:965–71
- Ehleringer JR, Hall AE, Farquhar GD, eds. 1993. *Stable Isotopes and Plant Carbon-Water Relations*. San Diego: Academic. 555 pp.
- Ekart DD, Cerling TE, Montañez IP, Tabor NJ. 1999. A 400 million year carbon isotope record of pedogenic carbonate: implications

- for paleoatmospheric carbon dioxide. *Am. J. Sci.* 299:805–27
- Evans JR, Sharkey TD, Berry JA, Farquhar GD. 1986. Carbon isotope discrimination measured concurrently with gas exchange to investigate CO₂ diffusion into leaves of higher plants. *Aust. J. Plant Physiol.* 13:281–92
- Falkowski P, Scholes RJ, Boyle E, Canadell J, Canfield D, et al. 2000. The global carbon cycle: a test of our knowledge of Earth as a system. *Science* 290:291–6
- Farquhar GD, O'Leary MH, Berry JA. 1982. On the relationship between carbon isotope discrimination and the intercellular carbon dioxide concentration in leaves. *Aust. J. Plant Physiol.* 9:121–37
- Farquhar GD, Ehleringer JR, Hubick KT. 1989. Carbon isotope discrimination during photosynthesis. *Annu. Rev. Plant Physiol. Mol. Biol.* 40:503–37
- Farquhar GD, Lloyd J. 1993. Carbon and oxygen isotope effects in the exchange of carbon dioxide between terrestrial plants and the atmosphere. See Ehleringer et al. 1993, pp. 47–70
- Farquhar GD, O'Leary MH, Berry JA. 1982. On the relationship between carbon isotope discrimination and the intercellular carbon dioxide concentration in leaves. *Aust. J. Plant Physiol.* 9:121–37
- Farquhar GD, von Cammerer S, Berry JA. 1980. A biochemical model of photosynthetic CO₂ assimilation in leaves of C3 species. *Planta* 149:78–90
- Feng X. 1998. Long-term c_i/c_a response of trees in western North America to atmospheric CO₂ concentration derived from carbon isotope chronologies. *Oecologia* 117:19–25
- Friedli H, Löffler H, Oeschger H, Siegenthaler U, Stauffer B. 1986. Ice core record of the ¹³C/¹²C ratio of atmospheric CO₂ in the past two centuries. *Nature* 324:237–38
- Ghosh P, Ghosh P, Bhattacharya SK. 2001. CO₂ levels in the Late Palaeozoic and Mesozoic atmosphere from soil carbonate and organic matter, Satpura basin, Central India. *Palaeogeog. Palaeoclim. Palaeoecol.* 170:219–36
- Gregory KM, Chase CG. 1992. Tectonic significance of paleobotanically estimated climate and altitude of the late Eocene erosion surface, Colorado. *Geology* 20:581–85
- Gröcke DR. 1998. Carbon-isotope analyses of fossil plants as a chemostratigraphic and palaeoenvironmental tool. *Lethaia* 31:1–13
- Gröcke DR, Hesselbo SP, Jenkyns HC. 1999. Carbon-isotope composition of Lower Cretaceous fossil wood: ocean-atmosphere chemistry in relation to sea-level change. *Geology* 27:155–58
- Guy RD, Fogel ML, Berry JA. 1993. Photosynthetic fractionation of the stable isotopes of oxygen and carbon. *Plant Physiol.* 101:37–47
- Harland WB, Armstrong RL, Cox AV, Craig LE, Smith AG, Smith DG. 1989. *A Geologic Timescale*. Cambridge: Cambridge Univ. Press. 263 pp.
- Hesselbo SP, Gröcke DR, Jenkyns HC, Bjerrum CJ, Farrimond P, et al. 2000. Massive dissociation of gas hydrate during a Jurassic anoxic event. *Nature* 406:392–95
- Hinrichs KU, Eglinton G, Engel MH, Summons RE. 2001. Exploiting multivariate isotopic nature of organic compounds. *Geochem. Geophys. Geosyst.* 2. Pap. No. 2001-GC000142
- Jahren AH, Arens NC, Sarmiento G, Guerrero J, Amundson R. 2001. Terrestrial record of methane hydrate dissociation in the Early Cretaceous. *Geology* 29:159–62
- Jones HG. 1992. *Plants and Microclimate*. Cambridge: Cambridge Univ. Press. 428 pp.
- Jones TP, Rowe NP, eds. 1999. *Fossil Plants and Spores: Modern Techniques*. London: Geol. Soc. 396 pp.
- Kaiho K, Arinobu T, Ishiwatari R, Morgans HEG, Okada H, et al. 1996. Latest Paleocene benthic foraminiferal extinction and environmental changes at Tawanui, New Zealand. *Paleoceanography* 11:447–65
- Keeling CD, Whorf TP, Wahlen M, van der Plicht J. 1995. Interannual extremes in the rate of atmospheric carbon dioxide since 1980. *Nature* 375:666–70
- Kennett JP, Stott LD. 1991. Abrupt deep-sea warming, palaeoceanographic changes and

- benthic extinctions at the end of the Palaeocene. *Nature* 353:225–29
- Kirchner JW, Weil A. 2000. Delayed biological recovery from extinctions throughout the fossil record. *Nature* 404:177–80
- Koch PL, Zachos JC, Dettman DL. 1995. Stable isotope stratigraphy and paleoclimatology of the Paleogene Bighorn Basin (Wyoming, USA). *Palaeogeog. Palaeoclim. Palaeoecol.* 115:61–89
- Koch PL, Zachos JC, Gingerich PD. 1992. Correlation between isotope records in marine and continental carbon reservoirs near the Palaeocene/Eocene boundary. *Nature* 358:319–22
- Körner Ch, Cochrane PM. 1985. Stomatal responses and water relations of *Eucalyptus pauciflora* in summer along an elevational gradient. *Oecologia* 66:443–55
- Krull ES, Retallack GJ. 2000. $\delta^{13}\text{C}$ depth profiles from paleosols across the Permian-Triassic boundary: evidence for methane release. *Geol. Soc. Am. Bull.* 112:1459–72
- Kump LK, Arthur MA. 1999. Interpreting carbon-isotope excursions: carbonates and organic matter. *Chem. Geol.* 161:181–98
- Kürschner WM, van der Burgh J, Visscher H, Dilcher DL. 1996. Oak leaves as biosensors of late Neogene and early Pleistocene palaeoatmospheric CO_2 concentrations. *Mar. Micropaleontol.* 27:299–312
- Kuypers MMM, Pancost RD, Damste JSS. 1999. A large and abrupt fall in atmospheric CO_2 during Cretaceous times. *Nature* 399:342–45
- Lake JA, Quick WP, Beerling DJ, Woodward FI. 2001. Signals from mature to new leaves. *Nature* 411:154
- Leavitt SW. 1993. Season $^{13}\text{C}/^{12}\text{C}$ changes in tree rings: species and site coherence, and a possible drought influence. *Can. J. For. Res.* 23:210–18
- Leavitt SW, Long A. 1986. Stable-carbon isotope variability in tree foliage and wood. *Ecology* 67:1002–10
- Leuning R. 1995. A critical appraisal of a combined stomatal-photosynthesis model for C_3 plants. *Plant Cell Environ.* 18:339–55
- Lloyd J, Farquhar GD. 1994. ^{13}C discrimination during CO_2 assimilation by the terrestrial biosphere. *Oecologia* 99:201–15
- Marshall JD, Monserud RA. 1996. Homeostatic gas-exchange parameters inferred from $^{13}\text{C}/^{12}\text{C}$ in trees of conifers. *Oecologia* 105:13–21
- McElwain JC. 1998. Do fossil plants signal palaeoatmospheric CO_2 concentration in the geological past? *Philos. Trans. R. Soc. London Ser. B* 353:83–96
- McElwain JC, Beerling DJ, Woodward FI. 1999. Fossil plants and global warming at the Triassic-Jurassic boundary. *Science* 285:1386–90
- McElwain JC, Chaloner WG. 1995. Stomatal density and index of fossil plants track atmospheric carbon dioxide in the Palaeozoic. *Ann. Bot.* 76:389–95
- McElwain JC, Chaloner WG. 1996. The fossil cuticle as a skeletal record of environmental change. *Palaios* 11:376–88
- McGuire AD, Melillo JM, Joyce DW, Kicklighter AL, Grace B, et al. 1992. Interactions between carbon and nitrogen dynamics in estimating net primary production for potential vegetation in North America. *Global Biogeochem. Cycles* 6:101–24
- Padden M, Weissert H, de Rafelis M. 2001. Evidence for Late Jurassic release of methane from gas hydrates. *Geology* 29:223–26
- Pálffy J, Demény A, Haas J, Hetényi M, Orchard MJ, Vető I. 2001. Carbon isotope anomaly and other geochemical changes at the Triassic-Jurassic boundary from a marine section in Hungary. *Geology* 29:1047–50
- Pearson PN, Palmer MR. 2000. Atmospheric carbon dioxide concentrations over the past 60 million years. *Nature* 406:695–99
- Petit JR, Jouzel J, Raynaud D, Barkov NI, Barnola J-M, et al. 1999. Climate and atmospheric history of the past 420,000 years from the Vostok ice core, Antarctica. *Nature* 399:429–36
- Poole I, Kürschner WM. 1999. Stomatal density and index: the practice. See Jones & Rowe, pp. 257–65
- Rees PA, Gibbs MT, Ziegler AM, Kutzbach JE,

- Behling PJ. 1999. Permian climates: evaluating model predictions using global paleobotanical data. *Geology* 27:891–94
- Retallack GJ. 2001. A 300-million-year record of atmospheric carbon dioxide from fossil plant cuticles. *Nature* 411:287–90
- Robertson I, Switsur AHC, Carter AHC, Barker AC, Waterhouse JS, et al. 1997. Signal strength and climate relationships in $^{13}\text{C}/^{12}\text{C}$ ratios of tree ring cellulose from oak in east England. *J. Geophys. Res. D* 102:19506–16
- Royer DL. 2001. Stomatal density and stomatal index as indicators of paleoatmospheric CO_2 concentration. *Rev. Palaeobot. Palynol.* 114:1–28
- Royer DL, Berner RA, Beerling DJ. 2001a. Phanerozoic CO_2 change: evaluating geochemical and paleobiological approaches. *Earth-Sci. Rev.* 54:349–92
- Royer DL, Wing SL, Beerling DJ, Jolley DW, Koch PL, et al. 2001b. Paleobotanical evidence for near present-day levels of atmospheric CO_2 during part of the Tertiary. *Science* 292:2310–13
- Rundgren M, Beerling D. 1999. A Holocene CO_2 record from the stomatal index of subfossil *Salix herbacea* L. leaves from northern Sweden. *Holocene* 9:509–13
- Schimmelmann A, DeNiro MJ. 1984. Elemental and stable isotope variations of organic matter from a terrestrial sequence containing the Cretaceous-Tertiary boundary at York Canyon, New Mexico. *Earth Plan. Sci. Lett.* 68:392–98
- Schoch PG, Zinsou C, Sibi M. 1980. Dependence of the stomatal index on environmental factors during stomatal differentiation in leaves of *Vigna sinensis* L. I. Effect of light intensity. *J. Exp. Bot.* 31:1211–16
- Sepkoski JJ. 1996. Patterns of Phanerozoic extinction: a perspective from global databases. In *Global Events and Event Stratigraphy in the Phanerozoic*, ed. OH Walliser, pp. 35–51. Berlin: Springer-Verlag
- Stott LD, Sinha A, Thiry M, Aubry M-P, Berggren WA. 1996. Global $\delta^{13}\text{C}$ changes across the Paleocene-Eocene boundary: criteria for terrestrial-marine correlations. *Geol. Soc. Spec. Pub.* 101:381–99
- Sundquist ET, Broecker WS, eds. 1985. *The Carbon Cycle and Atmospheric CO_2 : Natural Variations Archean to Present*. Monogr. 32. Washington, DC: Am. Geophys. Union
- Thackeray JF, van der Merwe NJ, Lee-Thorp JA, Sillen A, Lanham JL, et al. 1990. Changes in carbon isotope ratios in the late Permian recorded in the therapsid tooth apatite. *Nature* 347:751–53
- Tralau H. 1968. Evolutionary trends in the genus *Ginkgo*. *Lethaia* 1:63–101
- Van der Burgh J, Visscher H, Dilcher DL, Kürschner WM. 1993. Paleoatmospheric signatures in Neogene fossil leaves. *Science* 260:1788–90
- Veizer J, Ala D, Azmy K, Bruckschen P, Buhl D, et al. 1999. $^{87}\text{Sr}/^{86}\text{Sr}$, $\delta^{13}\text{C}$ and $\delta^{18}\text{O}$ evolution of Phanerozoic seawater. *Chem. Geol.* 161:59–88
- Wagner F, Bohncke SJP, Dilcher DL, Kürschner WM, van Geel B, Visscher H. 1999. Century-scale shifts in early Holocene atmospheric CO_2 concentration. *Science* 284:1971–73
- Walcroft AS, Silvester WB, Whitehead D, Kelliher FM. 1997. Seasonal change in stable carbon isotope ratios within annual rings of *Pinus radiata* reflect environmental regulation of growth processes. *Aust. J. Plant Physiol.* 24:57–68
- Walker JCG. 1994. Global geochemical cycles of carbon. In *Regulation of Atmospheric CO_2 and O_2 by Photosynthetic Carbon Metabolism*, ed. NE Tolbert, J Preiss, pp. 75–89. New York: Oxford Univ. Press. 272 pp.
- Ward PD, Haggart JW, Carter ES, Wilbur D, Tipper HW, Evans T. 2001. Sudden productivity collapse associated with the Triassic-Jurassic boundary mass extinction. *Science* 292:1148–51
- Wolbach WS, Gilmour I, Anders E, Orth CJ, Brooks RR. 1988. Global fire at the Cretaceous/Tertiary boundary. *Nature* 334:665–69
- Wolfe JA, Schorn HE, Forest CE, Molnar P.

1997. Paleobotanical evidence for high altitudes in Nevada during the Miocene. *Science* 276:1672–75
- Wong SC, Cowan IR, Farquhar GD. 1978. Leaf conductance in relation to assimilation in *Eucalyptus pauciflora* Sieb. ex Spreng. Influence of irradiance and partial pressure of carbon dioxide. *Plant Physiol.* 62:670–74
- Wong SC, Cowan IR, Farquhar GD. 1979. Stomatal conductance correlated with photosynthetic capacity. *Nature* 282:424–26
- Woodward FI. 1986. Ecophysiological studies on the shrub *Vaccinium myrtillus* L. taken from a wide altitudinal range. *Oecologia* 70:580–86
- Woodward FI. 1987. Stomatal numbers are sensitive to increases in CO₂ from pre-industrial levels. *Nature* 327:617–18
- Woodward FI. 1993. Plant responses to past concentrations of atmospheric CO₂. *Vegetatio* 104/105:145–55
- Woodward FI, Bazzaz FA. 1988. The responses of stomatal density to CO₂ partial pressure. *J. Exp. Bot.* 39:1771–81
- Woodward FI, Kelly CK. 1995. The influence of CO₂ concentration on stomatal density. *New Phytol.* 131:311–27
- Zachos J, Pagani M, Sloan L, Thomas E, Billups K. 2001. Trends, rhythms, and aberrations in global climate 65 Ma to present. *Science* 292:686–93
- Zachos JC, Arthur MA, Dean WE. 1989. Geochemical evidence for suppression of pelagic marine productivity at the Cretaceous-Tertiary boundary. *Nature* 337:61–64
- Zachos JC, Stott LD, Lohmann KC. 1994. Evolution of early Cenozoic marine temperatures. *Paleoceanography* 9:353–87